

NUMERICAL DESIGN CALCULATION OF STRUCTURAL STEEL WELDS

Abhishek Ghimire^{1*}, František Wald², Martin Vild³, and Jaroslav Kabeláč⁴

^{1,2}*Czech Technical University in Prague, Czech Republic*

³*Brno University of Technology, Czech Republic*

⁴*IDEA RS s.r.o., U Vodárny 3032/2a, Brno, Czech Republic*

Email: ^{1} abhishek.ghimire@fsv.cvut.cz, ² wald@fsv.cvut.cz, ³ vild.m@fce.vutbr.cz,*

⁴ jaromir.kabelac@ideastatica.com

DOI: <https://doi.org/10.59382/pro.intl.con-ibst.2023.ses1-20>

ABSTRACT: This paper focuses on designing fillet welds made from high-strength steel (HSS). It presents a numerical design calculation (NDC) method for assessing weld strength using the regular inclined shell element model (RISEM) in the finite element method (FEM). NDC uses FEM to design joints according to standardised procedures. The inclined shell element in RISEM represents the geometry and stiffness of welds, controlling its stresses in the plane. The paper recommends using a common inclined shell element with rigid links to accurately represent the geometry and rigidity of fillet welds. A new strength criterion is proposed based on stresses on the inclined shell element, using maximum equivalent stress as an indicator. Validation of the method is confirmed by comparing RISEM and test results using finite element (FE) simulation. Additionally, the weld resistance computed from the equation in prEN 1993-1-8:2020 is also in good agreement.

KEYWORDS: Numerical design calculation, regular inclined shell element model, high-strength steel, strength.

1. INTRODUCTION

High-strength steels (HSSs) have become more prevalent in the steel market in the past few years. Compared to the traditionally used steel grades, it performs well in tensile strength, toughness, and weldability. Steel yield strength is constantly growing due to the continual development of new production processes [1]. Many steel industries are working to develop light and slender constructions of steel structures having good welding characteristics and high ductility [2]. HSS is used in a wide range with a demand for lightweight design of structures with increased structural performance [3]. It has a lower deformation capacity, and with increasing the strength of steel, the loads that have to be transferred by the welded connections increase in the same way [4]. Structural integrity is one of the crucial aspects in many industrial sectors where welding is a primary technique for connection. It is necessary to ensure these welded connections' strength and sufficient ductility and toughness to redistribute stresses and internal forces when using HSS [5]. The strength of welded connections can be determined using classical or finite element analysis (FEA) based on the details described in the respective design guidelines [6]. Numerical modelling is a valuable tool in design practice, providing reliable

results on the proposed system and its components [7]. Recently developed modelling techniques mimic the geometry and rigidity of welds for fatigue design in structural steels. Using weld modelling techniques can significantly reduce the time and effort required in fatigue design. However, there currently needs to be well-established methods for determining the resistance of welds in structural steels using numerical design models. The present study addresses this issue by exploring determining welded connection resistance from HSS welds using FEM.

The main scope of current work is developing a realistic, advanced design model for determining the strength of fillet weld connections of HSSs for steel construction. In particular, the stresses acting on the weld profile are considered the most sensitive components of a welded connection, and the design model corresponds with it through FEM. The prEN 1993-1-14:2021 [8] outlines two methods for finite element analysis-based design: numerical design calculation (NDC) and numerical simulation (NS). The volume model is commonly used in research-oriented numerical analysis in FEM, while the shell model is preferred for design-oriented NDC. The NDC models are used to check the direct resistances of a structure or part of it for the static design check [8]. The study

proposes a new strength criterion for transverse and longitudinal fillet welded connections based on the NDC of HSS welds. The proposed strength criterion was validated through physical experiments and verified by current design equations. The proposed design model eliminates the challenges of the volume model and helps engineers accurately and efficiently determine the strength of welded connections from HSS in combination with FEM.

2. CURRENT DESIGN EQUATION

Extensive research has been conducted to establish appropriate design guidelines for welding connections in both ordinary and high-strength structural steel. In Europe, EN 1993-1-8:2006 [9] recommends using either the directional method or the mean stress method to calculate the strength of fillet welded connections. The directional method resolves forces transmitted by the weld into stress components, σ_{\perp} , σ_{\parallel} , τ_{\perp} and τ_{\parallel} assuming the throat section is the resisting and failing section (see Figure 1). Normal stresses and shear stress components are calculated from design loads, assuming uniform stress distribution in the weld throat. However, it is essential to note that normal stress σ_{\parallel} parallel to the axis is not considered when verifying the design resistance of the weld [9].

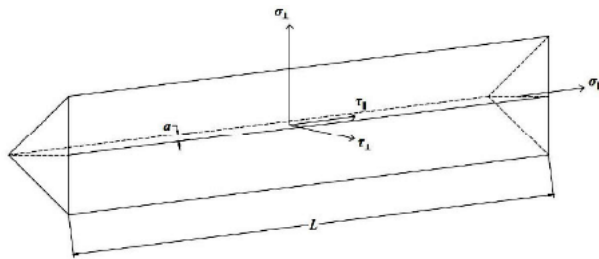


Figure 1. Stresses on the throat section of a fillet weld [9]

The most recent version of Eurocode prEN 1993-1-8:2020 [10] states that if the steel grade is S460 or higher, a fillet weld design resistance can be deemed adequate for connections with different base and filler metal strength, provided that a specific requirement is met.

$$\sqrt{\sigma_{\perp}^2 + 3\tau_{\perp}^2 + 3\tau_{\parallel}^2} \leq \frac{(0.25 f_{u,PM} + 0.75 f_{u,FM})}{\beta_{w,mod} \gamma_{M2}} \quad (1)$$

$$\text{and } \sigma_{\perp} \leq \frac{0.9 f_u}{\gamma_{M2}}$$

Where σ_{\perp} is the normal stress perpendicular to the throat, τ_{\perp} is the shear stress perpendicular to the axis of the weld, τ_{\parallel} is the shear stress parallel to the axis of the weld, $f_{u,PM}$ is the nominal ultimate

tensile strength of the parent metal, which is of lower strength grade, $f_{u,FM}$ is the nominal ultimate tensile strength of filler metal according to table 6.2 [10], $\gamma_{M2} = 1.25$ is the partial safety factor for the resistance of welds, $\beta_{w,mod}$ is the modified correlation factor that depends on the filler metal strength from Table 6.2 [10].

The design weld resistance of a connection with transverse fillet weld $F_{w,Rd,T}$ and longitudinal fillet weld $F_{w,Rd,L}$ can be determined by following functions:

$$F_{w,Rd,T} = \frac{(0.25 f_{u,PM} + 0.75 f_{u,FM})}{\sqrt{2} \beta_{w,mod} \gamma_{M2}} a.L \quad (2)$$

$$F_{w,Rd,L} = \frac{(0.25 f_{u,PM} + 0.75 f_{u,FM})}{\sqrt{3} \beta_{w,mod} \gamma_{M2}} a.L \quad (3)$$

Where a is the throat thickness of the weld and L is the length of weld. The length of longitudinal fillet welds in lap joint of steel grades equal to or greater than S460, is limited to $150 a$ [10].

3. EXPERIMENT

3.1. Specimen

The study analysed the strength and deformation capacity of transverse fillet lap-welded high-strength steel (HSS) connections. Steel plates 12 mm thick made from S700 MC Plus HSS and AristoRod

Table 1. Measured average mechanical properties of steel plates and weld metal

Material	Yield strength	Tensile strength	Ultimate strain (ε%)
	[MPa]	[MPa]	[-]
700 MC Plus	811.58	888.16	0.048
OK AristoRod 13.12	571.14	778.85	0.067

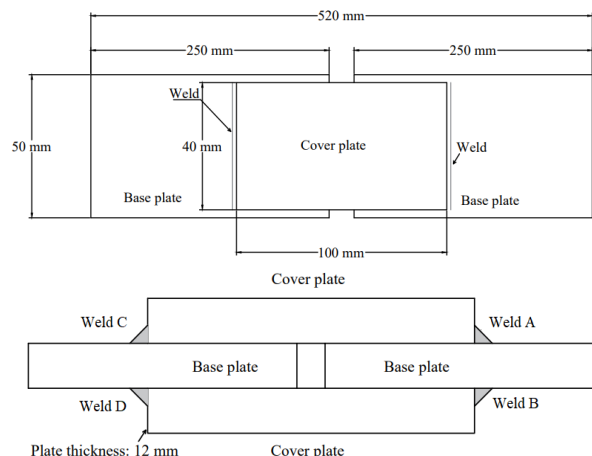


Figure 2. Transverse fillet lap-welded specimen

13.12 grade electrodes to create transverse fillet lap-welded connections. In order to analyse the properties of materials, conducted tests on four base metal tension coupons and three weld metal tension coupons following European Standards. The mechanical properties of the steel plates and weld metal coupons are presented in Table 1.

The typical geometry and configuration of a transverse fillet lap-welded connection are present in Figure 2. The mean measurements of the weld profile summarized in Table 3. A vernier calliper was used to determine the dimensions of plates and weld profiles. Six specimens with a transverse fillet lap-welded connection were created, with “TS” denoting the transverse specimen.

Table 3. Mean measurement before and after the experiment

Specimen	Weld		Total surface area	
	L [mm]	a [mm]	A_{th} [mm ²]	A_{fr} [mm ²]
TS-1	90	4.30	387.0	520.0
TS-2	90	3.15	283.5	338.0
TS-3	88	3.25	286.0	428.0
TS-4	88	3.45	303.6	398.0
TS-5	90	3.75	337.5	479.0
TS-6	88	3.30	290.4	473.0

3.2. Test execution

The test specimens underwent tensile loading with a maximum capacity of 1 MN in the machine. A specimen was set up in the testing machine to carry out the test, as shown in Figure 3. All tests are conducted with displacement control and a 1 mm/min loading rate. Displacement development and strain distribution during the loading process were measured using the digital image correlation (DIC) technique. Two cameras were used to capture measurements from both sides of the specimen’s target surface area, which had speckle patterns. Speckle patterns significantly impact the precision of image correlation since the recorded speckle patterns before and after a surface movement are necessary for the analysis. If necessary, a light projector facilitated lighting on the surface, as shown in Figure 3. The recorded measurements assessed the displacement and strain distribution of the transverse fillet weld.

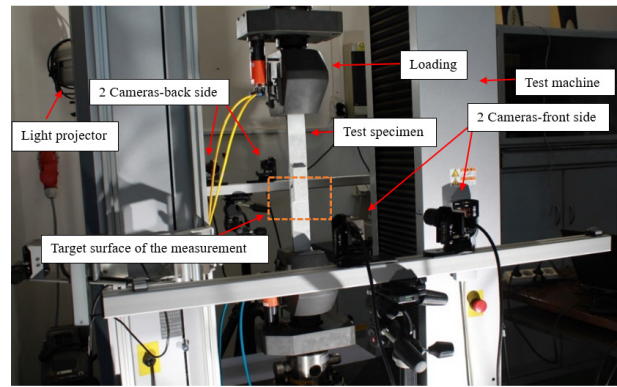


Figure 3. Setting of specimen on test machine

All transverse fillet lap-welded connections failed in the weld from both sides. The fracture surface area of the weld was measured by the photogrammetry method. In this process, the photos of the specimens were taken and created a 3D model of it. The target surface area of the weld was extracted from the 3D scanning analysis. The measured fracture surface area of the weld is present in Table 3.

3.3. Result

Experiments were conducted to determine the strength of transverse fillet welds by measuring their ultimate load capacity (F_u). Two welds are made on opposite sides of the base plate in a test specimen and are expected to share the ultimate load equally. The ultimate strength of the weld is calculated based on its failure surface area using theoretical throat area (A_{th}) and fracture surface area (A_{fr}). A_{th} is calculated by multiplying the length and throat thickness of the weld, while A_{fr} is the entire fracture surface area of the specimen after the test. The computed ultimate strength of the transverse weld (F_u/A_{th}) is based on the initial measurement of the weld profile, while the ultimate strength (F_u/A_{fr}) provides a real strength of the entire fracture surface.

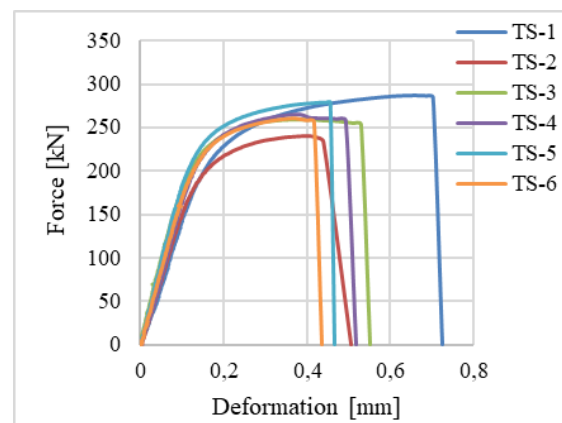


Figure 4. Force-deformation curve of transverse fillet lap-welded connection

Table 4. Mean strength and deformation of transverse fillet lap-welded connections from HSS

	Ultimate load	Strength		Deformation
	F_u [kN]	(F_u/A_{th}) [MPa]	(F_u/A_{fr}) [MPa]	δ_u [mm]
TS-1	287	742	552	0.66
TS-2	241	848	712	0.40
TS-3	259	906	605	0.37
TS-4	265	872	665	0.38
TS-5	279	827	582	0.45
TS-6	261	900	552	0.37

The deformation of the transverse fillet lap-welded connection was measured using DIC. The deformation of the fillet weld can be depicted by the relative displacement of two arbitrary points between the base and cover plate [11]. The process involved recording the relative displacement of two points and determining the corresponding strain. The force-deformation diagram of the transverse fillet lap-welded connections includes the relative displacement of points recorded by DIC measurement (see Figure 4). The summary of the mean strength and deformation of transverse fillet lap-welded connections from HSS presents in Table 4.

The effect of weld size on the ultimate strength of transverse fillet weld is presented graphically in Figure 5. There is no identical relationship between weld leg length and weld strength. However, the ultimate strength computed from the fracture surface area is less than that of using the theoretical area of the weld. This is because the fracture surface area is always higher than the theoretical area because, in most cases, the failure planes did not lie on the theoretical throat surface.

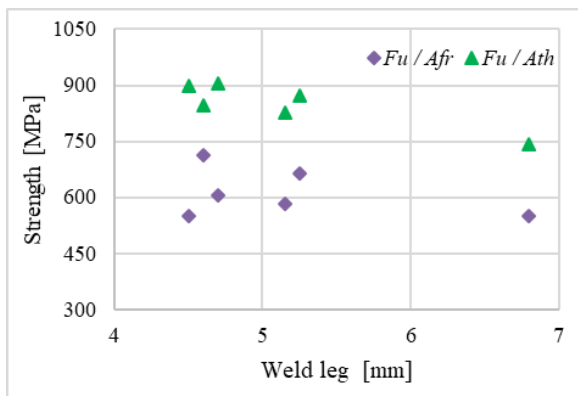


Figure 5. Ultimate strength of transverse fillet lap-welded specimen corresponds to the weld leg

4. NUMERICAL DESIGN CALCULATION (NDC)

The NDC uses numerical models to assess the strength of a structure or component during static design checks [8]. This study focuses on creating models of fillet welded connections using common inclined shell elements, known as regular inclined shell element models (RISEM), to analyse their direct weld resistances. This section outlines the design approach for proposing a new strength criterion for transverse and longitudinal fillet lap-welded connections made from high-strength steel (HSS) welds.

4.1. Regular inclined shell element model (RISEM)

4.1.1. General

RISEM uses finite shell elements to analyse plates and welds. The weld model aims to yield results similar to design codes with minimal computational requirements rather than simulating real-life behaviour. The calculations do not consider the residual stresses and weld shrinkage. An inclined shell element is utilised between multipoint constraints to represent the weld when analysing fillet welds. The element behaves according to the code's assumption that stresses are uniformly distributed in the weld throat, considering the thickness, location, and orientation of the weld throat.

4.1.2. Material information

When creating finite element models of structural steel, the most frequently used material diagrams are the ideal plastic, the elastic-plastic model with a small yielding plateau, the elastic model with strain hardening, and the stress-strain diagram that has been measured [8]. The RISEM model considers the nonlinear elastic-plastic properties of steel plates and welds, including a small yielding plateau. To calibrate the material model used in RISEM, standard coupon tests were conducted for both base and filler metals, as described in section 3.1.

4.1.3. Plate and weld model

In Abaqus, the plate and welds are represented by the shell element S4R, with six degrees of freedom in each node. These elements are positioned at the mid-plane of the real structural component [12], as demonstrated in Figure 6 a and 6 b. In this model, the inclined shell element represents welds and has the same thickness as the throat thickness of the weld. The thickness of other structural parts is defined as plate thickness. The base and cover plates are the master surface, while the inclined shell element is the slave surface.

These two surfaces are connected by a multipoint constraint rigid link, as illustrated in Figure 6b.

Using multi-point constraints has many advantages, such as allowing the connection of plates with different mesh densities and modelling plates with an offset, which considers the actual plate thicknesses and positions. The FE modelling involved analysing material nonlinearity behaviour using ABAQUS/CAE 6.14. The base plate was subjected to tensile load on one end, while the other had a fixed support boundary condition. The longitudinal edge of the base plate and cover plate were permitted to move only in the direction of the applied load, as shown in Figure 7.

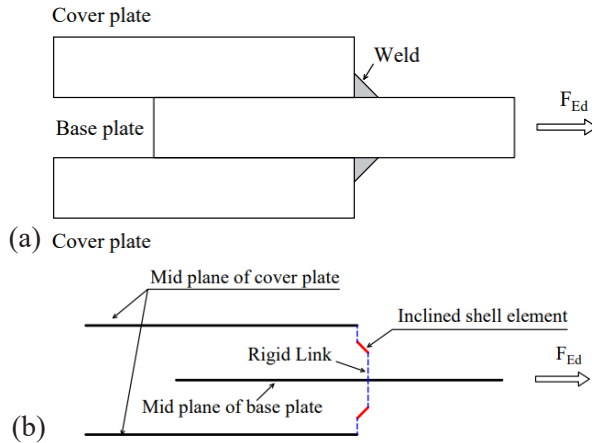


Figure 6. Sample cut with cross weld, (a) structural parts (b) mid plane of the structural parts with weld model

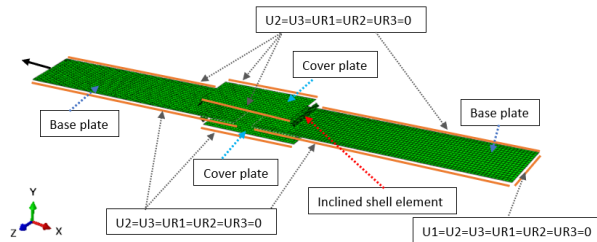


Figure 7. Regular inclined shell element model (RISEM) with boundary conditions

4.1.4. Mesh sensitivity study

A mesh sensitivity study involves using various grid resolutions in simulations to evaluate how the accuracy of solutions changes with each mesh. This study examines explicitly the inclined shell element, which plays a critical role in determining the design resistance of the welded connection. The mesh size is notably finer in the inclined shell element than in the base and cover plate, illustrated in Figure 7.

The number of elements along the length of the inclined shell elements varies from 20, 40, 80, and 134 in the case of transverse weld having a weld length of 40 mm, which corresponds to mesh size (MS): 2 mm \times 2 mm, 1 mm \times 1 mm, 0.5 mm \times 0.5 mm, 0.3 mm \times 0.3 mm, respectively. The

influence of the number of elements on the weld resistance presents in Figure 8. The black dashed lines represent the $\pm 5\%$ differences with the results of weld resistance by current design equations in prEN1993-1-8:2020 [10]. For more accurate calculations of weld resistance using RISEM and design equations [10], it is advisable to utilize a mesh size of 0.3 \times 0.3 mm along the length of the weld. This mesh size should be the $\frac{a}{10}$,

inclined shell element. The variable ‘a’ represents the throat thickness of the weld.

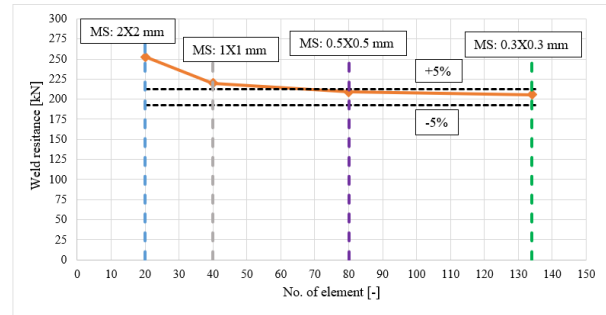


Figure 8. Influence of number of elements in the inclined shell elements on the weld resistance

4.2. A new design resistance function of fillet welded connections

This section describes the development of a novel method for determining the load-carrying capacity of transverse and longitudinal lap-welded connections. RISEM determines the resistance of fillet welds by considering the equivalent stresses on the inclined shell element. These stresses are obtained from FE shell models, where the element’s bottom surface experiences the maximum stress. The general principle of plane stress transformation equations in the inclined surface is considered to evaluate the equivalent stress. The theory of transformation of plane stress has been developed for a long time and is well explained in many material and mechanic textbooks [13]–[15].

When the force is perpendicular to the weld direction, the equivalent stress is determined by calculating the resultant of normal and shear stress that acts on the inclined shell element using the following function.

$$\sigma_{\text{eqv,FE}_T} = \sqrt{\sigma_n^2 + \tau_0^2} \quad (4)$$

Where $\sigma_{\text{eqv,FE}_T}$ is the equivalent stress acting on inclined shell element in FE shell model when line of action of the force is perpendicular to the weld direction, σ_n is the normal stress acting on inclined shell element, τ_0 is normal shear stress acting on inclined shell element.

$$\sigma_n = \frac{\sigma_x + \sigma_y}{2} - \left(\frac{\sigma_x - \sigma_y}{2} \right) \cos 2\theta - \tau_{yx} \sin 2\theta \quad (5)$$

$$\tau_\theta = \left(\frac{\sigma_x - \sigma_y}{2} \right) \sin 2\theta - \tau_{yx} \cos 2\theta \quad (6)$$

Similarly, suppose the line of action of the force is parallel to the weld direction. In that case, equivalent stress is calculated with the resultant of normal and parallel shear stress acting on the inclined surface from the following function:

$$\sigma_{eqv,EF_L} = \sqrt{\tau_p^2 + \tau_\theta^2} \quad (7)$$

Where σ_{eqv,EF_L} is the equivalent stress acting on inclined shell element in FE shell model when line of action of the force is parallel to the weld direction, τ_p is the shear stress acting parallel on inclined plane, and τ_θ is the normal shear stress on inclined plane.

$$\tau_p = \left(\frac{\sigma_x - \sigma_y}{2} \right) \sin 2\theta + \tau_{xy} \cos 2\theta \quad (8)$$

$$\tau_\theta = -\tau_{xy} \sin 2\theta \quad (9)$$

All stress components σ_x , σ_y , τ_{xy} , and τ_{yx} required for the normal stress, normal shear stress, and parallel shear stress on the inclined shell elements are computed from the RISEM in Abaqus. Similarly, the inclination of the inclined shell element θ is considered as per modelling of the specimens. The values are corresponding to σ_x is marked as S11, σ_y as S22, $\tau_{xy} = \tau_{yx}$ as S12 in RISEM.

The equivalent stresses acting on inclined shell elements evaluated with equations 4 and 7 are considered and limited as the maximum stresses of the weld in RISEM. The RISEM stresses are verified against the weld stresses calculated by analytical models in European standards [10]. The effective area of the weld is considered to calculate the weld resistance in both methods.

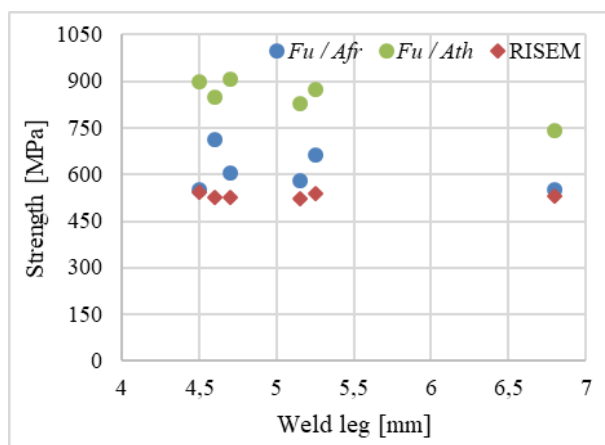


Figure 9. Comparison the strength with weld leg of transverse weld

4.3. Validation and verification

4.3.1. Validation of RISEM

This study compares the strength of transverse fillet lap-welded connections on various weld legs through two approaches: evaluating the strength based on the theoretical weld area and the fracture surface area of the weld (see Figure 9). It found that using the fracture surface area of the weld provides more accurate results, as it reflects the actual strength of the weld. The comparative results show that the calculated strength from RISEM and the actual strength from the test agreed well. In all cases, the test to-RISEM ratios were equal to or greater than 1.0, ranging from 1.0 to 1.29 (with a mean value of 1.13).

To ensure safety, the ultimate experimental strain of each specimen was compared to the effective strain from the RISEM. The RISEM weld model gives a conservative estimate of the ultimate strain (see Figure 10), which confirms that the welding techniques used in the design are safe.

Moreover, the validation of the proposed RISEM is presented based on the experimental works on HSS fillet welds in the following weld configuration.

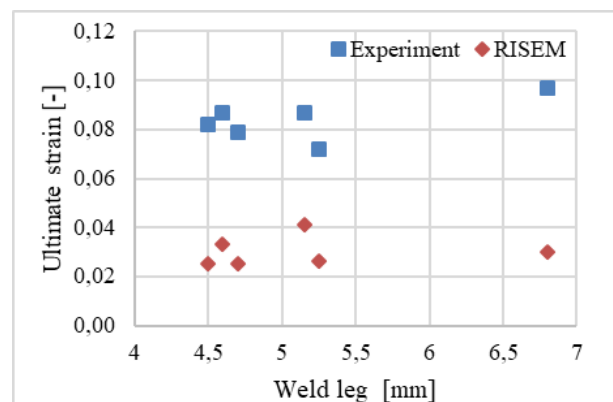


Figure 10. Comparison the ultimate strain with weld leg of transverse weld

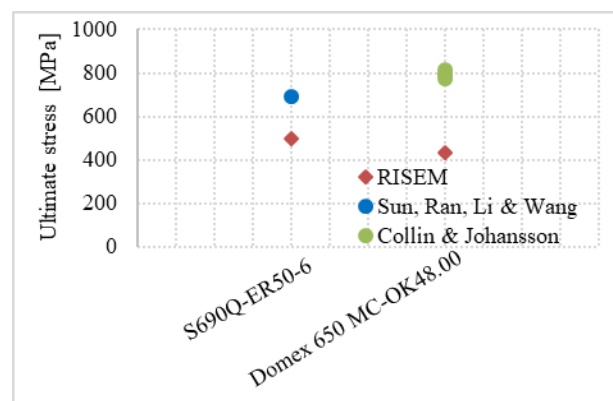


Figure 11. Comparison of strength from experiments and RISEM on transverse weld

1. Transverse welds (loaded in perpendicular): Collin and Johansson [16] and Sun, Ran, Li and Wang [11] examined the transverse fillet welded connection behaviour from HSS. The experiments involved lapped splice specimens with different welding consumables. The ultimate stress of transverse fillet welds computed from RISEM is

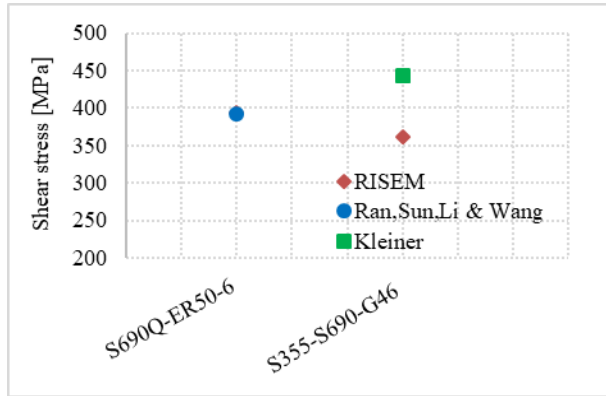


Figure 12. Comparison of strength from experiments and RISEM on longitudinal weld

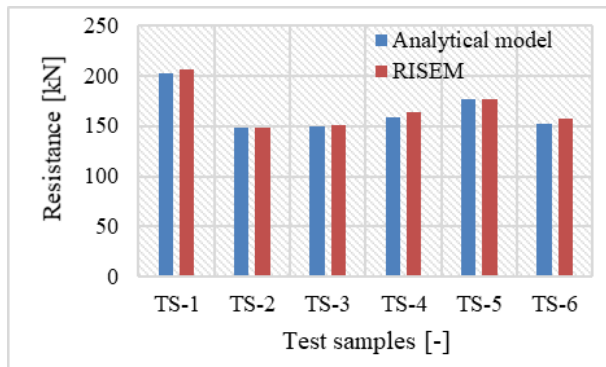


Figure 13. Comparison of the RISEM and analytical weld resistance of transverse fillet weld-CTU experiment

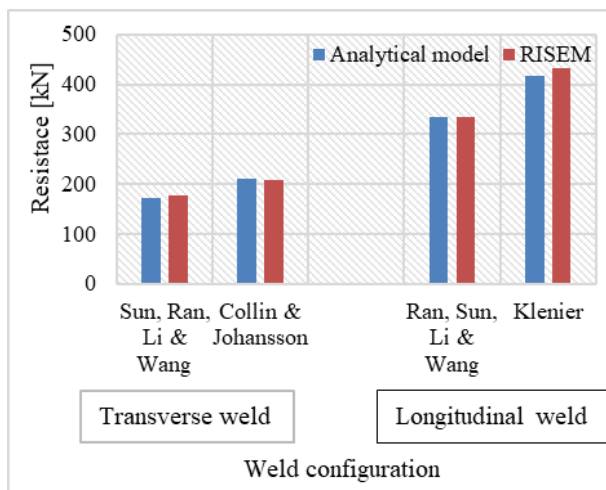


Figure 14. Comparison of the RISEM and analytical weld resistance of the transverse and longitudinal fillet welds- previous studies

conservative in both experimental results, as shown in Figure 11.

2. Longitudinal welds (loaded in parallel): Kleiner [17] and Ran, Sun, Li and Wang [18] experimented with various welding consumables on longitudinal welds. Compared to the observed behaviour in both experiments, the weld model used in RISEM leads to conservative estimations in terms of shear stress (see Figure 12) for an example with one welding electrode type from each experiment.

4.3.2. Verification of RISEM

In this study, the regular inclined shell element model (RISEM) resistance compared to the analytical resistance of weld calculated from the analytical model (AM) as per prEN1993-1-8:2020 [10]. The ultimate stresses acting in an inclined shell element were limited to compute the RISEM resistance.

The analytical model from the CTU experiment and RISEM results are presented in Figure 13, while Figure 14 compares RISEM results with analytical models prepared from previous studies. The RISEM resistance showed excellent agreement with analytical resistance in all cases, with a difference of less than 5%. This difference is acceptable for the design purpose of the weld.

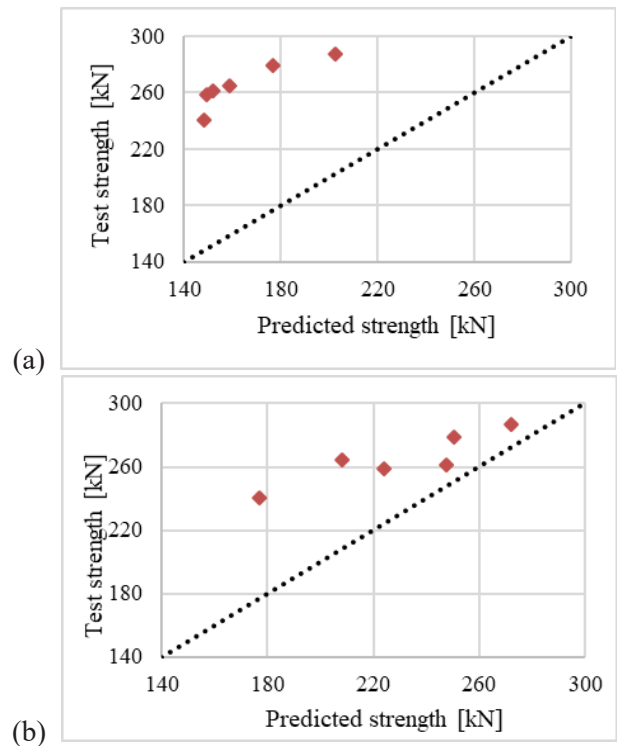


Figure 15. Test vs Predicted strength by (a) theoretical area of weld and (b) Fracture surface area of weld

5. COMPARISON WITH THE CURRENT DESIGN EQUATION

The weld strength of transverse fillet welds in Figure 15 compares with the test strength and the predicted strength by the current design equation [10]. During the calculation of weld strength by the current design equation, the ultimate strength of the filler and base materials was taken from the coupon test, along with a correlation factor from Table 6.2 [10] - a safety factor of 1.0 implemented to ensure an objective comparison.

The test strength is more conservative than the predicted strength based on the weld's effective theoretical and fracture surface area. The test-to-predicted ratios by effective theoretical area vary from 1.42 to 1.73 (mean value is 1.62) (see Figure 15a), while by fracture surface area vary from 1.06 to 1.36 (mean value is 1.17) (see Figure 15b). The predicted strength of the weld computed using the fracture surface area of the weld provides a better prediction value.

6. SUMMARY

This paper introduces numerical design calculation (NDC), which uses the regular inclined shell element model (RISEM) to analyse plates and welds. RISEM utilises finite shell elements to provide reliable results comparable to design codes with minimal computational requirements rather than simulating real-life behaviour. RISEM is verified against analytical models in prEN1993-1-8:2020 and validated through physical tests of HSS fillet welds loaded in different directions. The RISEM method is recommended for NDC of HSS fillet weld resistance and ductility for design purposes based on computed results, and the following observations and conclusions are made:

- Using the fracture surface area provides a more accurate representation of the weld's strength than the effective theoretical area. The failure of the weld does not usually occur along the throat section.

- The NDC determines weld resistance by limiting ultimate stresses in a RISEM. Results from experiments indicate that the weld resistance of RISEM aligns with the analytical models in prEN1993-1-8:2020, with only a 6% variance.

- RISEM's weld model is conservative in estimating ultimate strain, ensuring the suitability of welding techniques for design purposes.

- RISEM test strength ratios are consistently 1.0 to 1.29 (average 1.13), similar to predicted ratios in the current design equation (average 1.17).

ACKNOWLEDGEMENTS

The study was supported by TAČR grant [FW01010392], and the paper was supported by grant no. SGS22/141/OHK1/3T/11 from CTU in Prague.

REFERENCE

- [1] Saufnay, L., Jaspard, J., & Demonceau, J. (2021). *Economic benefit of high strength steel sections for steel structures*. Ce/Papers, 4(2-4): 1543-1550. doi: 10.1002/cepa.1454.
- [2] Spiegler, J., & Kuhlmann, U. (2018). *Innovative high-strength steel construction using mixed connections*. Steel Construction, 11(4): 272-277.
- [3] Khurshid, M., Barsoum, Z., & Mumtaz, N. A. (2012). *Ultimate strength and failure modes for fillet welds in high strength steels*. Journal of Materials, 40: 36-42. doi: 10.1016/j.matdes.2012.03.048.
- [4] Kuhlmann, U., Günther, H.-P., & Rasche, C. (2008). *High-strength steel fillet welded connections*. Steel Construction, 1(1): 77-84. doi: 10.1002/stco.200890013.
- [5] Günther, H. P., Hildebrand, J., Rasche, C., Christian, V., Wudtke, I., Kuhlmann, U., ... & Werner, F. (2012). *Welded connections of high-strength steels for the building industry*. Welding in the World, 56: 86-106.
- [6] Griskevicius, P., Urbas, M., Capas, V., & Kozlovas, A. (2011). *Modeling of Welded Connections in SolidWorks Simulation*. Proceedings of the 16th International Conference - Mech. 2011: 104-108.
- [7] Krejsa, M., Brozovsky, J., Mikolasek, D., Parenica, P., Koubova, L., & Materna, A. (2017). *Numerical Modeling of Fillet and Butt Welds in Steel Structural Elements with Verification Using Experiment*. Procedia Engineering, 190: 318-325. doi: 10.1016/j.proeng.2017.05.344.
- [8] prEN 1993-1-14. (2021). EN 1993-1-14 – *Eurocode 3: Design of steel structures – Part 1-14: Design assisted by finite element analysis (Draft)*.
- [9] European Committee for Standardization (CEN). (2005). *Eurocode 3: Design of steel structures - Part 1-8: Design of joints, European Standards*, CEN, 50, 77.
- [10] European Standards. (2020). prEN 1993-1-8:2020 Eurocode 3-Design of steel structures-Part 1-8: Design of joints, (March).

- [11] Sun, F. F., Ran, M. M., Li, G. Q., & Wang, Y. B. (2019). *Mechanical behavior of transverse fillet welded joints of high strength steel using digital image correlation techniques*. Journal of Constructional Steel Research, 162: 105710. doi: 10.1016/j.jcsr.2019.105710.
- [12] Hobbacher, A. (2008). *Recommendation for fatigue design of welded joints and components*. International Institute of Welding (IIW).
- [13] Meyers, M. A., & Chawla, K. K. (2008). *Mechanical behavior of materials*. Cambridge university press.
- [14] Beer, P. F., Johnston, E. R., DeWolf, J. T., & Mazurek, D. F. (2012). *Mechanics of materials*. McGraw-Hill.
- [15] Philpot, T. A., Hall, R. H., Hubing, N., Flori, R., Oglesby, D. B., & Vikas, Y. (2003). *Animated instructional media for stress transformations in a mechanics of materials course*. Computers & Applied Engineering Education, 11(1): 40-52. doi:10.1002/cae.10037.
- [16] Collin, P., & Johansson, B. (2005). *Design of welds in high strength steel*. In European Conference on Steel and Composite Structures: 08/06/2005-10/06/2005 (pp. 4-10). Verlag Mainz.
- [17] Kleiner, A. (2018). *Beurteilung des Tragverhaltens von Flankenkehlnahtverbindungen aus normal- und höherfestem Baustahl unter Berücksichtigung statistischer Kriterien*.
- [18] Ran, M. M., Sun, F. F., Li, G. Q., & Wang, Y. B. (2021). *Mechanical behaviour of longitudinal lap-welded joints of high strength steel: Experimental and numerical analysis*. Thin-Walled Structures, 159: 107286. doi: 10.1016/j.tws.2020.107286.